


# Root presence modifies the long-term decomposition dynamics of fungal necromass and the associated microbial communities in a boreal forest

François Maillard<sup>1,2</sup>  | Peter G. Kennedy<sup>2</sup> | Bartosz Adamczyk<sup>3</sup> | Jussi Heinonsalo<sup>4,5,6</sup> | Marc Buée<sup>1</sup>

<sup>1</sup>INRAE, UMR IAM, Université de Lorraine, Nancy, France

<sup>2</sup>Department of Plant and Microbial Biology, University of Minnesota, St. Paul, MN, USA

<sup>3</sup>Natural Resources Institute Finland, Helsinki, Finland

<sup>4</sup>Department of Microbiology, University of Helsinki, Helsinki, Finland

<sup>5</sup>Institute for Atmospheric and Earth System Research (INAR)/Forest Sciences, University of Helsinki, Helsinki, Finland

<sup>6</sup>Finnish Meteorological Institute, Helsinki, Finland

## Correspondence

François Maillard, Department of Plant and Microbial Biology, University of Minnesota, St. Paul, MN, USA.  
Email: francois.maillard2@gmail.com

## Abstract

Recent studies have highlighted that dead fungal mycelium represents an important fraction of soil carbon (C) and nitrogen (N) inputs and stocks. Consequently, identifying the microbial communities and the ecological factors that govern the decomposition of fungal necromass will provide critical insight into how fungal organic matter (OM) affects forest soil C and nutrient cycles. Here, we examined the microbial communities colonising fungal necromass during a multiyear decomposition experiment in a boreal forest, which included incubation bags with different mesh sizes to manipulate both plant root and microbial decomposer group access. Necromass-associated bacterial and fungal communities were taxonomically and functionally rich throughout the 30 months of incubation, with increasing abundances of oligotrophic bacteria and root-associated fungi (i.e., ectomycorrhizal, ericoid mycorrhizal and endophytic fungi) in the late stages of decomposition in the mesh bags to which they had access. Necromass-associated  $\beta$ -glucosidase activity was highest at 6 months, while leucine aminopeptidase activity was highest at 18 months. Based on an asymptotic decomposition model, root presence was associated with an initial faster rate of fungal necromass decomposition, but resulted in higher amounts of fungal necromass retained at later sampling times. Collectively, these results indicate that microbial community composition and enzyme activities on decomposing fungal necromass remain dynamic years after initial input, and that roots and their associated fungal symbionts result in the slowing of microbial necromass turnover with time.

## KEYWORDS

bacteria, boreal forest soil, carbon cycling, ectomycorrhizal fungi, ericoid mycorrhizal fungi, fungal necromass, fungi, mycelium turnover

## 1 | INTRODUCTION

Boreal ecosystems represent one of Earth's largest carbon (C) sinks (Crowther et al., 2016; Pan et al., 2015). In boreal forests, organic matter is mainly accumulated in the upper layers of the soil, where

it forms a significant C stock (Lehmann & Kleber, 2015). Soil organic matter (SOM) accumulation depends on the rate of decomposition of above- and belowground litters, for which microbes play a central role (Kyaschenko et al., 2017; Kyaschenko et al., 2017; Sun et al., 2018). Although the decomposition dynamics of aboveground

plant-derived OM have received decades of attention, Clemmensen et al. (2013) demonstrated that belowground litters, such as roots and root-associated fungi, contributed up to 70% of the SOM pool in boreal forest soils. Dead fungal mycelium in particular, hereafter referred to as fungal necromass, has been estimated to represent more than 25% of the soil organic C (Liang et al., 2019) and up to 40% of stabilised nitrogen (N) in forest soils (Wang et al., 2020). While the initial decomposition of fungal necromass is typically fast (days to weeks; Brabcová et al., 2016; Fernandez et al., 2019; Ryan et al., 2020), Fernandez et al. (2019) found that in boreal peatland forest soils decomposition quickly reached a stable plateau that persisted for multiple years. That empirical result is consistent with other studies (e.g., Clemmensen et al., 2013; Liang et al., 2019) showing that microbial necromass can be a significant component of the soil stable C pool. In addition, due to its substantial amounts of the amino-sugar chitin, fungal biomass is relatively rich in N (Wallander et al., 2003) compared to plant-derived OM (Cools et al., 2014). For this reason, fungal necromass decomposition also probably plays a significant role in the N cycle in boreal soils, which often have low N accessibility (Högberg et al., 2017; Näsholm et al., 2009).

At both local and regional scales, the decomposition rate of the fungal necromass has been shown to be strongly affected by its biochemical quality (Beidler et al., 2020; Brabcová et al., 2018; Maillard et al., 2020). In particular, fungal necromass decomposition rate is known to be positively correlated with initial N concentration (Brabcová et al., 2018; Fernandez & Koide, 2012, 2014; Koide & Malcolm, 2009). In contrast, increases in melanin content, a pigment found in ~2/3 of soil fungal species (Siletti et al., 2017), have been shown to consistently decelerate fungal necromass decomposition (Ekblad et al., 2013; Fernandez & Kennedy, 2018; Fernandez & Koide, 2014; Fernandez et al., 2019). To explain the initially high decomposition rates of fungal necromass followed by a plateau phase, Fernandez et al. (2019) suggested that fungal necromass consists of two primary pools; a fast nutrient pool constituted of easily degradable compounds and a slow pool composed of recalcitrant compounds (i.e., melanin). This biphasic decomposition pattern has been validated with experimental data in other studies (Adamczyk et al. 2019; Brabcová et al., 2016, 2018; Drigo et al., 2012; Schweigert et al., 2015). Additional biotic and abiotic factors that have been found to significantly influence the turnover rates of fungal necromass in soils include mycelium morphology (Certano et al., 2018; Koide et al., 2014), soil temperature and site microtopography (Fernandez et al., 2019), and the presence of plant-derived tannins (Adamczyk, Sietiö, Biasi, et al., 2019).

Whereas identifying the factors determining rates of fungal necromass decomposition is increasingly well characterised, detailed description of the microbial communities associated with necromass decomposition have been more limited. Bacterial and fungal communities colonising fungal necromass during the first stages (up to 5 months) of incubation were recently described in both North American (Beidler et al., 2020; Fernandez & Kennedy, 2018; Maillard et al., 2020) and European forests (Brabcová et al., 2016, 2018). The bacterial communities associated with fungal

necromass decomposition were notably consistent between those studies, being dominated by copiotrophic bacteria belonging to phyla Proteobacteria and Bacteroidetes (Beidler et al., 2020; Brabcová et al., 2016, 2018; Fernandez & Kennedy, 2018). The fungal communities associated with fungal necromass were mostly composed either by Ascomycota or Mucoromycota saprotrophic fungi (Brabcová et al., 2016, 2018; Maillard et al., 2020), although Basidiomycota ectomycorrhizal fungi (ECM) were also present to varying degrees. The presence of this latter fungal guild is somewhat surprising, given that ECM fungi generally tend to be abundant in later stages of OM decomposition (Rajala et al., 2012, 2015; Voříšková & Baldrian, 2013). Ecological and physiological results, however, support the hypothesis that some ECM fungi are able to mine organic N from plant-derived OM (Bödeker et al., 2014; Nicolás et al., 2019; Rineau et al., 2012; and for a synthesis see Kuyper, 2017) and transfer protein-derived N to host plant (Akroume et al., 2019; Heinonsalo et al., 2015). Additionally, other studies using enzymatic approaches have also suggested that ECM fungi might be able to degrade fungal-derived OM (Buée et al., 2007; Hodge et al., 1995; Maillard et al., 2018; Mucha et al., 2006).

Despite significant recent progress in the study of fungal necromass decomposition, most studies to date have focused only on short-term mass loss (weeks) and the early-colonising microbial communities associated with decaying necromass. Given the long-term persistence of the more recalcitrant fractions of fungal necromass, it is unclear to what extent those fractions remain actively colonised by microbial decomposers. Additionally, very few studies have measured the enzymes associated with the decomposition on fungal necromass, which, together with sequence-based identification, can help determine the resources targeted by different groups of microbial decomposers. Finally, there is increasing recognition that roots play a major role in determining the trajectory of soil OM decomposition (Adamczyk, Sietiö, Straková, et al., 2019). Specifically, roots can hasten rates of OM decay through C inputs (i.e., rhizosphere priming; Kuzyakov, 2010) or retard OM decomposition through the release of inhibitory compounds such as tannins (Adamczyk, Sietiö, Biasi, et al., 2019). Finally, limitations on root presence may significantly impact the abundance of various root-associated microbes, including ECM fungi, which may themselves slow OM decomposition rates via selective resource utilisation (Frey, 2019).

Here, we studied the multiyear dynamics of fungal necromass decomposition in a Finnish Scots pine boreal forest. Specifically, we examined the same mesh bags containing fungal necromass as Adamczyk, Sietiö, Biasi, et al. (2019), but conducted three novel analyses. First, we used high-throughput sequencing to identify the bacterial and fungal communities associated with fungal necromass decomposition after 6, 18, and 30 months of soil incubation. Second, we quantified activities of three enzymes ( $\beta$ -glucosidase, leucine aminopeptidase and N-acetylglucosaminidase) targeting distinct C and N components of fungal necromass at the same sampling times. Third, we reanalysed the fungal necromass mass loss rates to assess the potentially different impacts of root presence at earlier versus later sampling times. We hypothesised that both the bacterial and

fungal community composition would shift over the course of the incubation, favouring oligotrophic bacteria and mycorrhizal fungi at later sampling times. We also predicted higher enzyme activities earlier in the incubation, with a more gradual decrease in the enzymes involved in chitin and peptide than polysaccharide degradation. Finally, we anticipated that the presence of roots may initially stimulate fungal necromass decomposition due to rhizosphere priming effects, but that over time, root-associated microbes, particularly mycorrhizal fungi, may retard mass loss through selective resource utilisation.

## 2 | MATERIALS AND METHODS

### 2.1 | Study site

The study was performed at Hyytiälä Forestry field station (61°51'N, 24°17'E) of the University of Helsinki and SMEAR II (Station to Measure Ecosystem-Atmosphere Relation: Hari & Kulmala, 2005), which is a Class I Ecosystem and Atmospheric station of ICOS Finland. The forest is dominated by ~60-year-old Scots pine (*Pinus sylvestris* L.) with an understory of Norway spruce (*Picea abies* L.) and scattered Silver birch (*Betula pendula* L.) (Ilvesniemi et al., 2000). *Vaccinium vitis-idaea* L. and *V. myrtillus* L. are dominant shrubs and *Hylocomium splendens* Hedw. and *Pleurozium schreberi* Brid. dominant mosses in the ground vegetation (Ilvesniemi et al., 2000). The soil has podzol horizons, typical to boreal coniferous forests. Within this stand, three subplots having a radius of 10 m and separated by a minimum distance of ~50 m were established for the fungal necromass incubations.

### 2.2 | Fungal necromass preparation, incubation and final quantification

The decomposition of fungal hyphal biomass was determined using mesh bags filled with 3 g dry weight (DW) of dead fungal biomass. The biomass originated from a basidiomycete *Chondrostereum purpureum*, cultivated in a large-scale (150 L) fermentor at 25°C, pH 5.5 in malt extract (25–35 g/L) and yeast extract (10 g/L). *Chondrostereum purpureum* was chosen because of its fast growth rate allowing for rapid production of fungal necromass. Biomass was first washed with excess distilled water, then dried in +80°C for 72 h to kill the mycelium, and then coarsely ground into pieces larger than 1 mm. The necromass was placed into three different kinds of nylon mesh bags (10 × 10 cm) constructed with mesh sizes of 1, 50 and 1000 µm. The smallest mesh size was meant to allow bacterial colonisation but preclude external fungal hyphal penetration, whereas 50 µm mesh size was meant to allow external fungal hyphal penetration, and the 1000 µm mesh size was meant to allow both external fungal hyphal and root penetration. As such, these differing mesh sizes created three levels of potential plant and microbial influence on decomposition: 1 µm mesh allowing only saprotrophic bacterial decomposition,

50 µm mesh allowing both saprotrophic bacterial and fungal as well as ectomycorrhizal fungal decomposition, and 1000 µm mesh allowing all microbial saprotrophic decomposition as well as plant-root associated microbes and plant roots. Mesh bags (hereafter referred to as mycobags) were buried between organic and topmost mineral soil horizons in May 2013 and harvested after 6 months, 18 months, and 30 months. Within each sub-plot, the different mesh sizes were placed close to each other, composing "a set" of bags. These sets of bags were separated by 5 m. Locations were randomised but not placed closer than 1 m to a tree. After removal, soil from external parts of the mycobags were cleaned. Plant roots were removed, and we controlled for soil contamination (see Adamczyk, Sietiö, Biasi, et al., 2019 for further details). The fresh and dry weight of mycobag content were measured and mass loss determined. Here, we randomly chose 12 of the 24 initial replicates for the subsequent analyses for each of the 9 different treatments.

### 2.3 | Molecular analyses

We extracted total nucleic acids from 40 mg of dry fungal necromass ( $n = 108$  samples) using the DNeasy PowerSoil Kit (Qiagen) following the manufacturer's instructions. To identify the bacterial community, we amplified the V4 region of the 16S SSU rRNA with the forward 515F (5'-GTGCCAGCMGCCGCGGTAA) and reverse 806R (5'-GGACTACHVHHHTWTCTAAT) primers (Caporaso et al., 2012). We carried out amplification on 1 µl of template DNA in a volume of 25 µl using Taq PCR Master Mix Kit (Qiagen). The program was as follow: 3 min at 94°C, 35 cycles of 1 min at 95°C, 1 min 50°C and 1 min at 72°C, and a final step 10 min at 72°C. We made the PCR reactions for each sample in triplicate, and PCR products were confirmed using gel electrophoresis and pooled. We amplified fungal ITS2 region, recognised as DNA barcode for fungal identification, with the forward gITS7 (5'-GTGARTCATCGARTCTTTG) and reverse ITS4 (5'-TCCTCCGCTTATTGATATGC) primers (Ihrmark et al., 2012). We carried out amplification on 1 µl of template DNA in a volume of 25 µl using Taq PCR Master Mix Kit (Qiagen). The program was as follow: 3 min at 94°C, 35 cycles of 1 min at 95°C, 1 min 52°C and 1 min at 72°C, and a final step 10 min at 72°C. We did the PCR reactions for each sample in triplicate and PCR products were confirmed using gel electrophoresis and pooled. Bacterial and Fungal libraries were sequenced using MiSeq 2 × 250 bp V2 Illumina chemistry by the GeT-PlaGe platform (INRAE).

For both the bacterial and fungal communities, paired sequences were demultiplexed according to their tags, primers were removed, and filtered (Quality score 30). Shorter sequences (<200 bp), as well as chimeric sequences and singletons were removed based on prediction by Uchime, USEARCH v8.0.1616 software (Edgar, 2013). Dereplication and clustering were performed with USEARCH software. Operational taxonomic units (OTUs) were generated at 97% similarity threshold for both bacteria and fungi. ITS2 sequences lacking a fungal kingdom classification were removed, and plant sequences proportion were calculated. Given

the limited exclusion of the plant sequences by the gITS7-ITS4 primer pair (Li et al., 2020), we assessed the root exclusion efficiency of the different mesh size treatments by comparing the proportion of ITS2 sequences belonging to plant. Bacterial and fungal data sets were rarefied to 7820 and 8097 sequences per sample, respectively (Figure S1). Three bacterial and two fungal samples that presented a low number of total sequences were removed prior to the rarefaction step. The number of replicates for each treatment is summarised in Table S1. For bacteria, a representative sequence of each OTU was taxonomically assigned using SILVA release 132 (Pruesse et al., 2007) at a confidence threshold of 97%. Taxonomic assignment of representative sequences for each fungal OTU was done using the Basic Local Alignment Search Tool (BLAST) algorithm v2.2.23 (Altschul et al., 1990) against the UNITE database Version 7.2 (Kõljalg et al., 2013; UNITE Community, 2017). Control samples of nonincubated necromass were included to identify the OTU corresponding to *C. purpureum*. DNA was extracted, and libraries were prepared exactly as described previously. ITS2 of the initial fungal necromass corresponded to OTU 10 and was detected at an extremely low relative abundance and frequency at all sampling times, depending on the mesh size (Figure S2). Because of this very low presence we decided not to exclude these sequences.

Bacterial OTUs were assigned to copiotrophic and oligotrophic modes based on Trivedi et al. (2018). Specifically, all bacterial OTUs belonging to the phylum Bacteroidetes and classes alpha-Proteobacteria, beta-Proteobacteria and gamma-Proteobacteria were defined as copiotrophs, while bacterial OTUs belonging to phylum Acidobacteria and class delta-Proteobacteria were defined as oligotrophs. Trophic mode assignments for fungi were made with FUNGuild (Nguyen et al., 2016). Symbiotrophic assigned OTUs were separated into endophyte, ericoid mycorrhizal fungi and ECM fungi. Remaining fungal OTUs belonging to Eurotiales, Hypocreales, Mortierellales, Saccharomycetales, Tremellales and Sporidiales as well as fungal OTUs defined by FUNGuild as microfungi, yeasts, and facultative yeasts were classified as moulds and yeasts, following Sterkenburg et al. (2015). OTUs presenting multiple lifestyles were regrouped as "other".

## 2.4 | Enzymatic analyses

The extracellular enzymes present in mesh bags were collected using the filter centrifugation method described in Heinonsalo et al. (2012). Activities of N-acetylglucosaminidase (EC 3.2.1.14),  $\beta$ -glucosidase (EC 3.2.1.21), and leucine aminopeptidase (EC 3.4.11.1) were measured using a fluorometric substrate assay as in Courty et al. (2005). The reactions were carried out at 22°C at pH 4.5, except for leucine aminopeptidase where pH 6.5 was used. The fluorescence signals were detected with a Victor3 plate reader (Perkin Elmer) using excitation at 355 nm and emission at 460 nm. Fluorescence standard curves were prepared from 4-methylumbelliferone, or aminomethylcoumarin in case of leucine aminopeptidase. Readings from buffers

and substrates only were used as background and subtracted from samples values.

## 2.5 | Decay rate modelling

Due to the well-recognised nonlinear nature of OM decomposition (Berg, 2014), we assessed fungal necromass mass loss rates using multiple nonlinear exponential decay models. We compared exponential decay fits for necromass in each treatment with and without an asymptote. The best fitting models, which included a decay constant ( $k$ ), a scaling factor ( $1 - A$ ) and an asymptote ( $A$ ), were selected based on a lower Bayesian Information criterion (BIC) score and higher  $r^2$  value, as detailed in Fernandez et al. (2019). This modelling was done using JMP 14 Pro.

## 2.6 | Statistical analysis

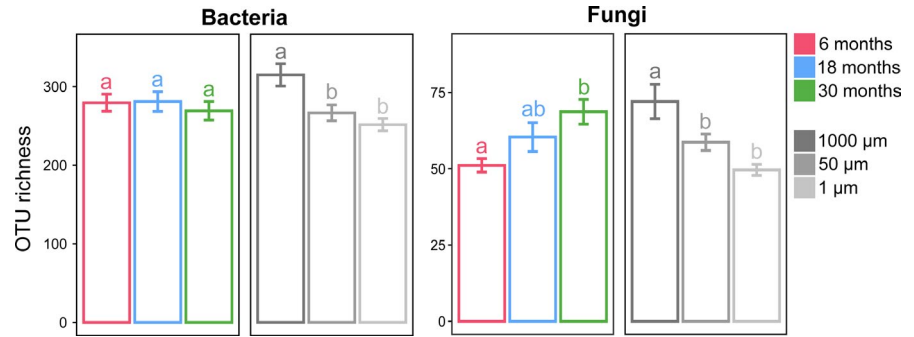
Statistical and graphical analyses were performed using R software (R Core Team, 2016) on bacterial and fungal rarefied counts. OTU richness was calculated with the vegan package (Oksanen et al., 2013). We evaluated time and mesh size effect on mass remaining and enzyme activities using two-way analyses of variance (ANOVA). Variance homoscedasticity was tested using Cochran's test, and data were log-transformed if necessary. We evaluated time and mesh size effect on OTU richness using two-way ANOVA. Differences in soil bacterial and fungal OTUs composition were visualised with nonmetric multidimensional scaling (NMDS) plots based on Bray-Curtis dissimilarity matrix using the metaMDS function in vegan. Permutational multivariate analysis of variance (PERMANOVA) based on Bray-Curtis dissimilarity was applied to determine time and mesh size treatment effect on bacterial and fungal OTU composition. We evaluated time and mesh size effect on bacterial and fungal guilds relative abundance and OTU richness using two-way ANOVAs. Similarly, for the most abundant bacterial and fungal genera (those representing a cumulative sum of 80% of mean relative abundance for both bacterial and fungal communities), we also used two-way ANOVAs to measure the effect of time and mesh size for each bacterial and fungal genus. Pearson's correlations were used between the most abundant bacterial and fungal genera and the necromass mass remaining at the different time points (6, 18 and 30 months).

# 3 | RESULTS

## 3.1 | Bacterial communities associated with fungal necromass

Following quality filtering and rarefaction, we retained 105 samples representing a total of 821,100 sequences belonging to 1322 bacterial OTUs. Bacterial OTU richness was relatively stable

**FIGURE 1** Bacterial and fungal OTU richness (mean ± SE) depending on incubation time (6, 18 and 30 months) or mesh size (1000, 50 and 1 μm); bars that do not share similar letters denote statistical significance ( $p \leq .05$ )



across all three harvests (Figure 1; Table S2). Bacterial community OTU richness was significantly higher in the 1000 μm mycobags by 18% and 25% by comparison with respectively the 50 and 1 μm mycobags ( $F_{2,96} = 8.523, p < .001$ ). No significant time × mesh size interaction effects were measured for bacterial OTU richness (Table S2).

NMDS analysis revealed that the bacterial community colonising 50 μm and 1 μm mycobags were more similar in terms of OTU composition by comparison with the 1000 μm mycobags at the 6 and 18 month sampling times, but that the 50 μm mesh size treatment tended to converge with the 1000 μm mycobags bacterial community after 30 months (Figure 2a). Time of incubation was the main factor governing the bacterial community structure, explaining 20.3% of variation in OTU composition ( $F_{2,96} = 13.499, p < .001$ ) (Figure 2b, Table S3). When mesh size treatments were analysed separately, the effect of time remained the main factor explaining the bacterial community composition. The effect of mesh size was also significant ( $F_{2,96} = 2.853, p < .001$ ), but explained only 4.3% of the variation in the bacterial community composition. When time treatments were analysed separately, the mesh size treatment had a significant effect on bacterial OTU composition at 18 and 30 months but not at 6 months.

The bacterial community consisted primarily of Acidobacteria, Actinobacteria, alpha-, gamma- and delta-Proteobacteria, Bacilli, Bacteroidia, and Verrucomicrobiae (Figure 2c). Alpha-Proteobacteria, gamma-Proteobacteria and Bacteroidia represented the most abundant classes colonising the fungal necromass after 6 months of incubation, with Acidobacteriia, Actinobacteria, Bacilli and Verrucomicrobiae increasing gradually to become the most dominant classes after 30 months of incubation. No effect of mesh size was found on the bacterial classes relative abundance.

The overall composition of the bacterial guilds colonising fungal necromass was dominated by copiotrophic bacteria at all three sampling times (Figure 3a). However, time of incubation significantly affected both copiotrophic ( $F_{2,96} = 69.519, p < .001$ ) and oligotrophic bacteria relative abundances ( $F_{2,96} = 10.952, p < .001$ ) (Table S4), with the former decreasing from 60% to 20% over time and the latter increasing from 2.5% at 6 months to 8% at 30 months. In addition, copiotrophic bacteria were significantly more abundant in 1 μm mycobags than in 1000 μm mycobags (Figure 3a,  $F_{2,96} = 3.195, p < .05$ ). Similar analyses conducted on OTU richness mirrored the relative abundance patterns, with copiotrophic OTU richness significantly

increasing ( $F_{2,96} = 29.021, p < .001$ ) and oligotrophic OTU richness decreasing ( $F_{2,96} = 14.231, p < .001$ ) over incubation time (Figure S3a,b, Table S4).

Most of the abundant bacterial genera colonising fungal necromass were significantly impacted by the incubation time (Figure 4). *Chitinophaga*, *Dokdonella*, *Ferruginibacter*, *Mucilaginibacter*, and *Pedobacter* were among the most abundant bacterial genera after 6 months of incubation and then declined throughout the experiment. Conversely, some bacterial genera were not abundant at the 6 month harvest, but significantly increased at the 18 and 30 month harvests, including *Bacillus*, *Cohnella*, *Granulicella*, *Mycobacterium* and *Paenibacillus*. Furthermore, *Acidothermus*, *Bradyrhizobium*, *Burkholderia*, *Cohnella*, and *Mycobacterium* were significantly enriched in 1000 μm mesh size treatment by comparison with the 50 and 1 μm mesh size treatments. Other genera such as *Achromobacter*, *Dokdonella*, *Dyella* and *Orchrobactrum* were significantly more abundant in 50 and 1 μm mycobags by comparison with 1000 μm mycobags. *Cohnella*, *Labilithrix*, *Paenibacillus* and *Rhodococcus* relative abundances were significantly negatively correlated with the amount of fungal necromass remaining. Conversely, *Acidipila*, *Dyella*, *Flavobacterium*, *Streptacidiphilus* and *Streptomyces* relative abundances were significantly positively correlated with the amount of fungal necromass remaining.

### 3.2 | Fungal communities associated with fungal necromass

Following quality filtering and rarefaction, we retained 106 samples representing a total of 858,282 sequences belonging to 655 fungal OTUs. Fungal community OTU richness ( $F_{2,97} = 6.173, p < .01$ ) increased over time, being significantly lower at the 6 month harvest than the 30 month harvest (Figure 1, Table S2). In contrast, fungal community OTU richness decreased depending on the mesh size, with significantly lower richness ( $F_{2,97} = 10.593, p < .001$ ) in both the 50 and 1 μm mycobags compared to the 1000 μm mycobags.

NMDS analysis revealed that fungal communities colonising fungal necromass in 50 and 1 μm mycobags had similar OTU composition and clustered separately compared with the 1000 μm mycobags fungal communities (Figure 2d). Both incubation time ( $F_{2,97} = 3.248, p < .001$ ) and mesh size ( $F_{2,97} = 2.549, p < .01$ ) significantly affected fungal community composition, respectively, explaining 5.7% and



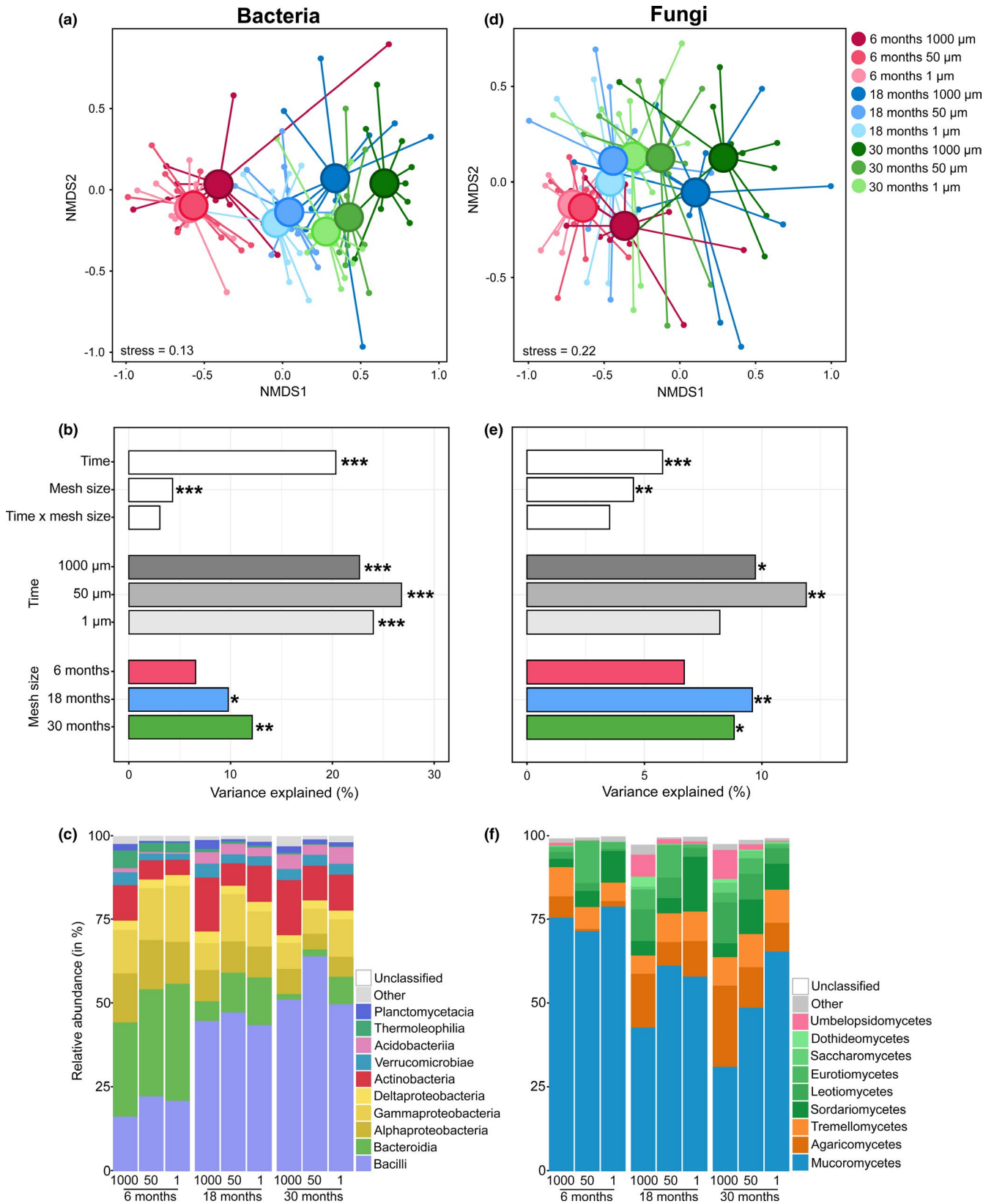
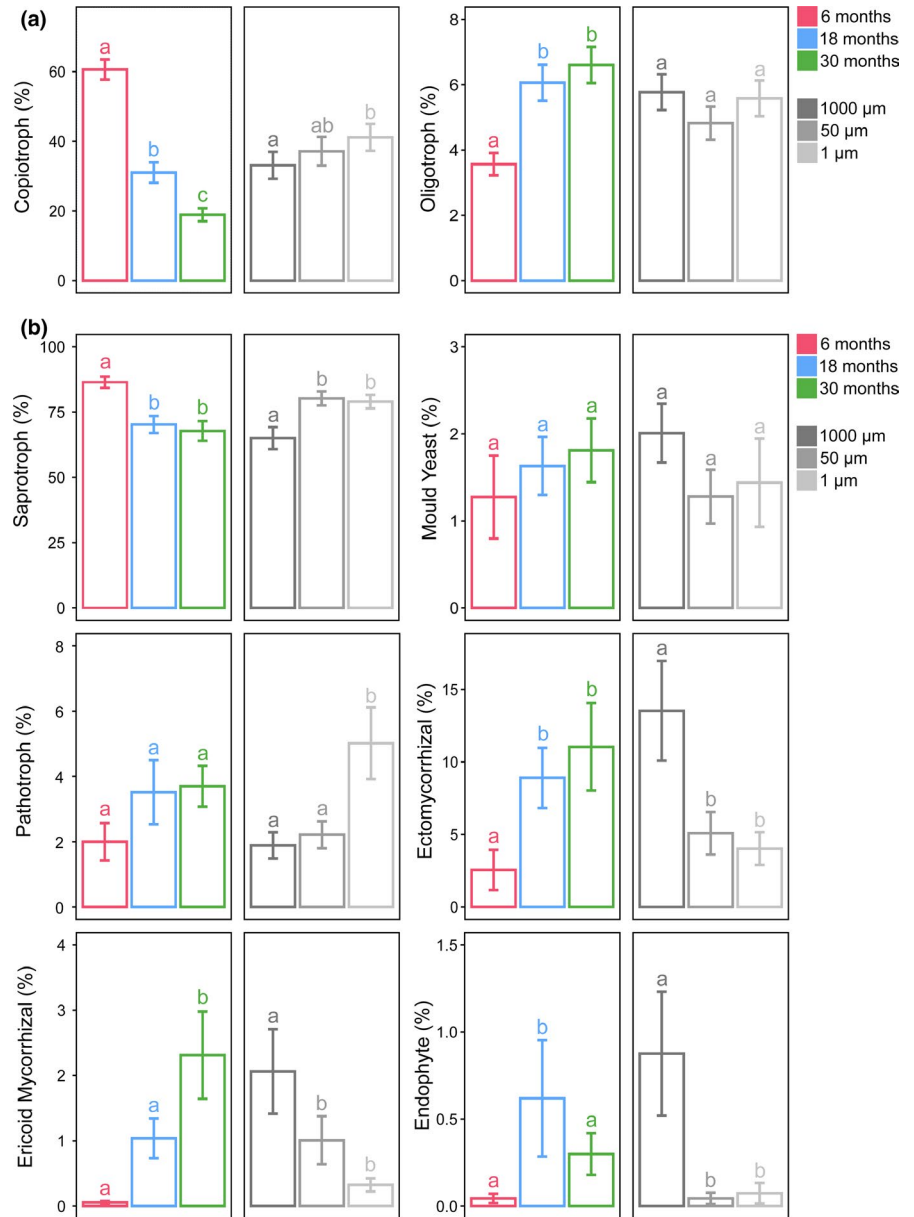


**FIGURE 2** Nonmetric multidimensional scaling (NMDS) analysis of the (a) bacterial and (d) fungal communities based on OTU composition depending on incubation time (6, 18 and 30 months) and mesh size (1000, 50 and 1 μm). Variance explained in (b) bacterial and (e) fungal OTU composition based on Permutational multivariate analysis of variance (PERMANOVA) depending on incubation time (6, 18 and 30 months) and mesh size (1000, 50 and 1 μm), and for incubation time and mesh size treatments alone. The relative abundances of (c) bacterial and (f) fungal classes colonising the fungal necromass depending on incubation time (6, 18 and 30 months) and mesh size (1000, 50 and 1 μm)

**FIGURE 3** Relative abundances of (a) bacterial and (b) fungal functional guilds (mean ± SE) depending on incubation time (6, 18 and 30 months) or mesh size (1000, 50 and 1 µm); bars that do not share similar letters denote statistical significance ( $p \leq .05$ )



4.5% of variation in OTU composition (Table S3). A separate analysis of incubation time revealed that the time effect was lower for fungal community in the 1 µm mycobags by comparison with the 50 and 1000 µm mycobags (Figure 2e). Differences in mesh size did not significantly affect fungal OTU composition at 6 months, but did at 18 and 30 months (Figure 2b).

Throughout all sampling time points, the fungal community was strongly dominated by the class Mucoromycetes (up to 75% relative abundance depending on the mesh size) followed by the Agaricomycetes, Eurotiomycetes, Leotiomyces, Sordariomycetes and Tremellomycetes (Figure 2f). Mucoromycetes relative abundance decreased depending on time mostly in the 1000 µm mycobags, whereas this class remained dominant in the 50 and 1 µm mycobags throughout the experiment. Conversely, there was a sharp increase in the classes Agaricomycetes and Umbelopsidomycetes at the 18 and 30 month sampling times in the 1000 µm mycobags.

Saprotrophs represented the dominant fungal guild colonising the fungal necromass across all harvests (Figure 3b). Saprotrophic fungal abundance decreased depending on harvest time ( $F_{2,97} = 12.641, p < .001$ ) (Table S4). In contrast, the relative abundances of ECM fungi ( $F_{2,97} = 4.433, p < .05$ ) and ericoid mycorrhizal (ERM) fungi ( $F_{2,97} = 9.121, p < .001$ ) significantly increased over time. In addition, ECM fungi ( $F_{2,97} = 6.331, p < .01$ ), ERM fungi ( $F_{2,97} = 5.936, p < .01$ ) and endophytic fungi ( $F_{2,97} = 5.739, p < .01$ ) were more all abundant in 1000 µm mesh size treatment than in 50 and 1 µm treatments mycobags, whereas an opposite trend was present for both saprotrophic ( $F_{2,97} = 9.033, p < .001$ ) and pathotrophic fungi ( $F_{2,97} = 5.755, p < .01$ ). OTU richness of ECM fungi ( $F_{2,97} = 10.291, p < .001$ ), ERM fungi ( $F_{2,97} = 25.782, p < .001$ ) and endophytic fungi ( $F_{2,97} = 3.891, p < .05$ ) significantly increased over time (Figure S3a,b, Table S4). In 1000 µm mesh size, OTU richness of ECM fungi ( $F_{2,97} = 3.207, p < .05$ ), ERM fungi ( $F_{2,97} = 13.707,$

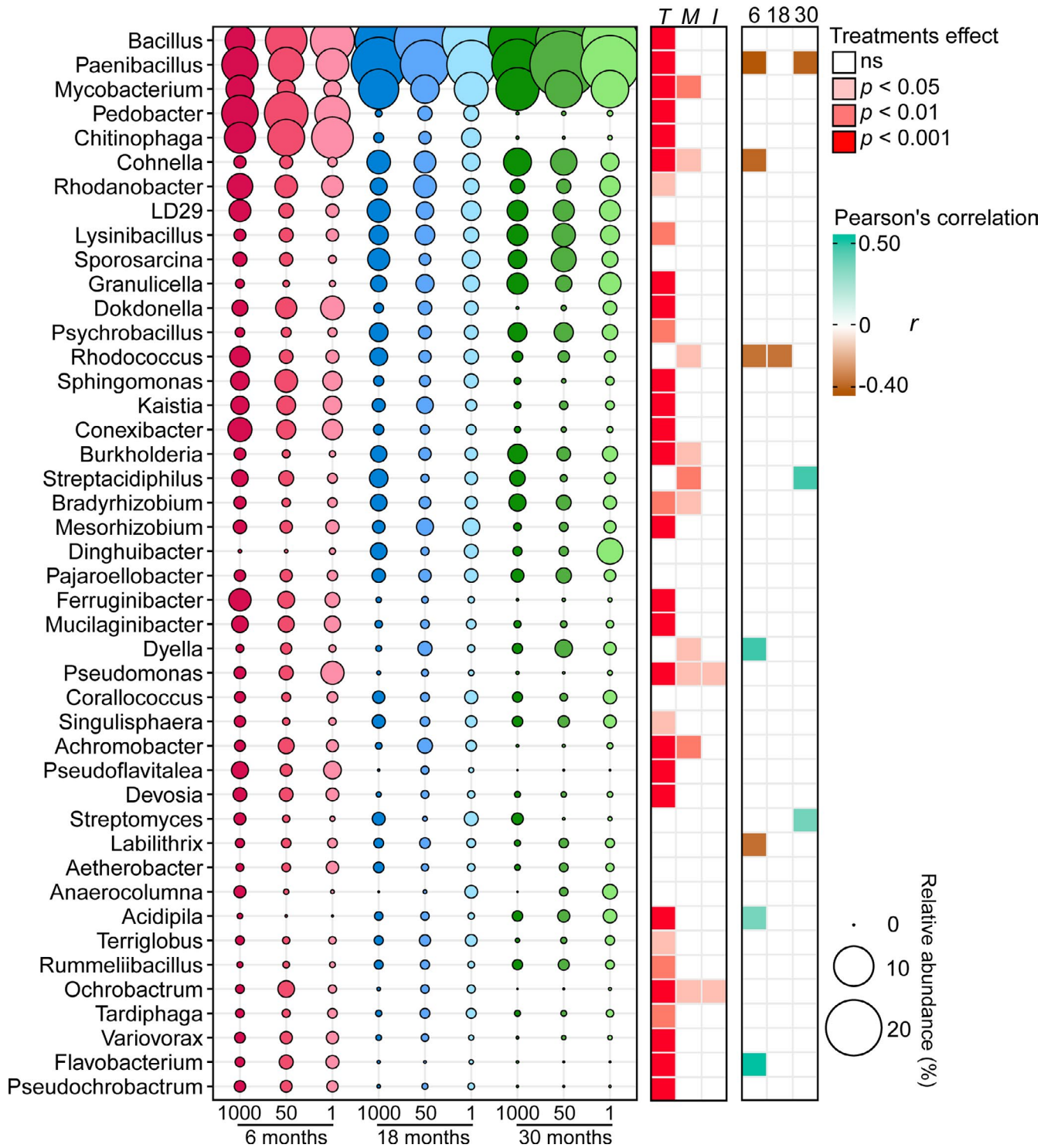


**FIGURE 4** Bacterial genera relative abundance depending on incubation time (6, 18 and 30 months) and mesh size (1000, 50 and 1  $\mu\text{m}$ ). The more abundant bacterial genera contributing to 80% of the total relative abundance are represented. The size of the circles is related to the relative abundance of each bacterial genus. The influence of incubation time (6, 18 and 30 months) and mesh size (1000, 50 and 1  $\mu\text{m}$ ) on the relative abundances of each bacterial genus was evaluated using two-way ANOVA and  $p$ -value are summarised in red (T = Time, M = Mesh size, I = Time  $\times$  Mesh size); ns refers to nonsignificant results. Pearson's correlations between bacterial genera relative abundance and fungal necromass mass remaining at different sampling times (6, 18 and 30 months). Only significant correlations are shown ( $p \leq .05$ )

$p < .01$ ), and endophytic fungi ( $F_{2,97} = 20.917$ ,  $p < .001$ ) was significantly higher than than in 50 and 1  $\mu\text{m}$  mycobags (Figure S3a,b, Table S4).

*Mucor* was the most abundant fungal genus throughout the experiment, but significantly decreased in later harvests (Figure 5). *Mucor* relative abundance was also significantly lower in 1000  $\mu\text{m}$  mycobags at



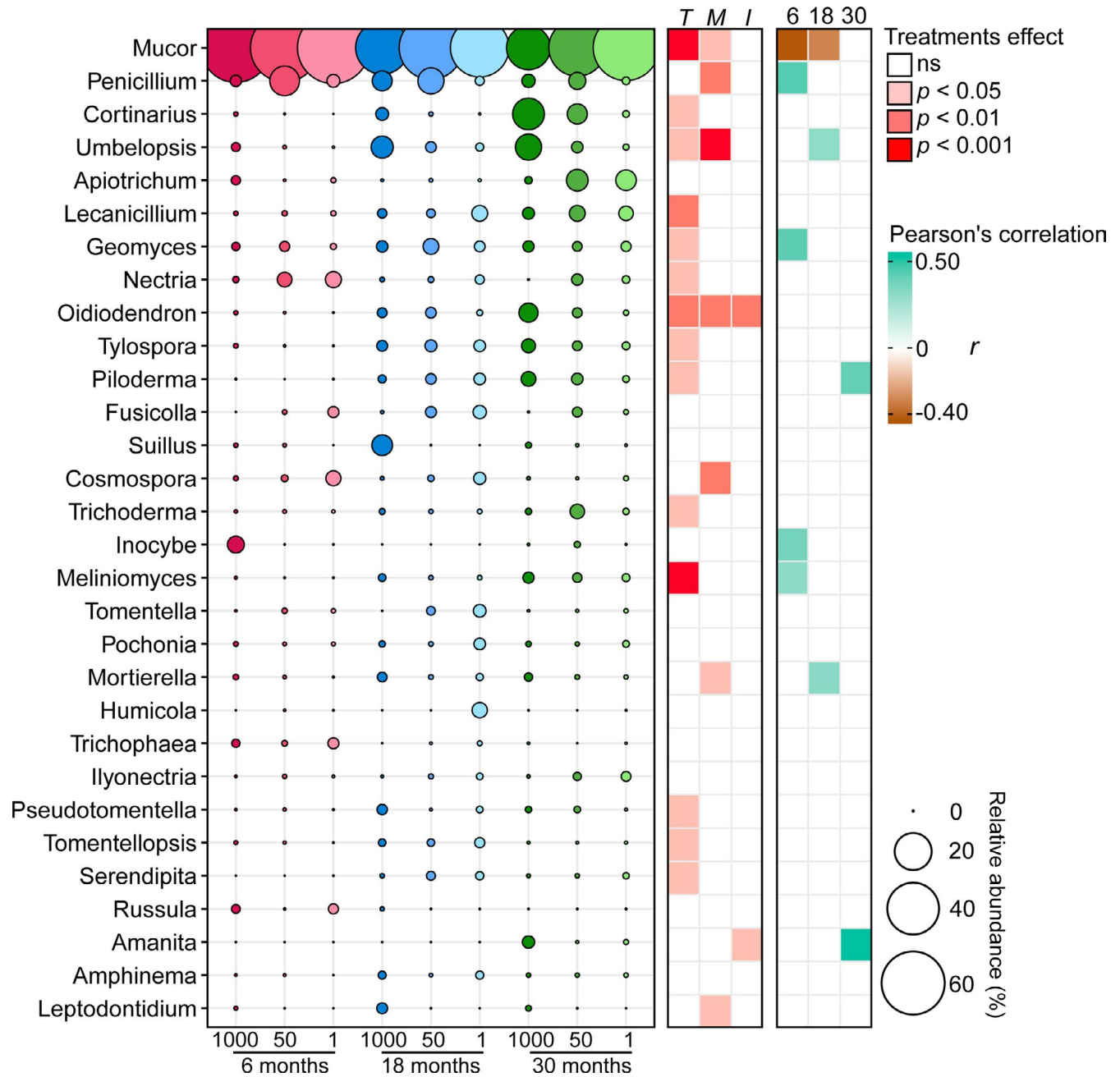


**FIGURE 5** Fungal genera relative abundance depending on incubation time (6, 18 and 30 months) and mesh size (1000, 50 and 1 µm). The more abundant fungal genera contributing to 80% of the total relative abundance are represented. The size of the circles is related to the relative abundance of each fungal genus. The influence of incubation time (6, 18 and 30 months) and mesh size (1000, 50 and 1 µm) on the relative abundances of each fungal genus was evaluated using two-way ANOVA and  $p$ -value are summarised in red (T = Time, M = Mesh size, I = Time × Mesh size); ns refers to nonsignificant results. Pearson's correlations between fungal genera relative abundance and mass remaining at different sampling times (6, 18 and 30 months). Only significant correlations are shown ( $p \leq .05$ )

the 18 and 30 month sampling times compared to with the 50 and 1 µm mycobags. Additionally, *Mucor* relative abundance was significantly negatively correlated with the amount of fungal necromass remaining. In contrast, the second most abundant fungal genus, *Penicillium*, was significantly more abundant in the 50 µm mycobags than either the 1000 or 1 µm mycobags. The fungal genera *Apiotrichum*, *Cortinarius*, *Lecanicillium*, *Oidiodendron*, *Piloderma*, *Tylospora* and *Umbelopsis*

increased significantly with time, and the 1000 µm mycobags were significantly enriched in *Cortinarius*, *Oidiodendron* and *Umbelopsis*. In addition, *Geomyces*, *Inocybe*, *Meliniomyces* and *Penicillium* were significantly positively correlated with the fungal necromass mass remaining at the 6 month sampling time, while *Amanita*, *Mortierella*, *Piloderma* and *Umbelopsis* were positively correlated with the amount of fungal necromass remaining at later sampling times.

### 3.3 | Enzymatic activities associated with fungal necromass

$\beta$ -glucosidase activity was significantly impacted by the time of incubation ( $F_{2,96} = 10.674$ ,  $p < .001$ ) (Table S5), being higher at 6 months than at either 18 or 30 months (Figure 6). Leucine aminopeptidase activity was also significantly influenced by the time of incubation ( $F_{2,96} = 12.268$ ,  $p < .001$ ), reaching a maximum after 18 months. In contrast, N-acetylglucosaminidase activity was not significantly impacted by incubation time and none of the three enzymatic activities were significantly affected by the mesh size treatment (Figure 6).

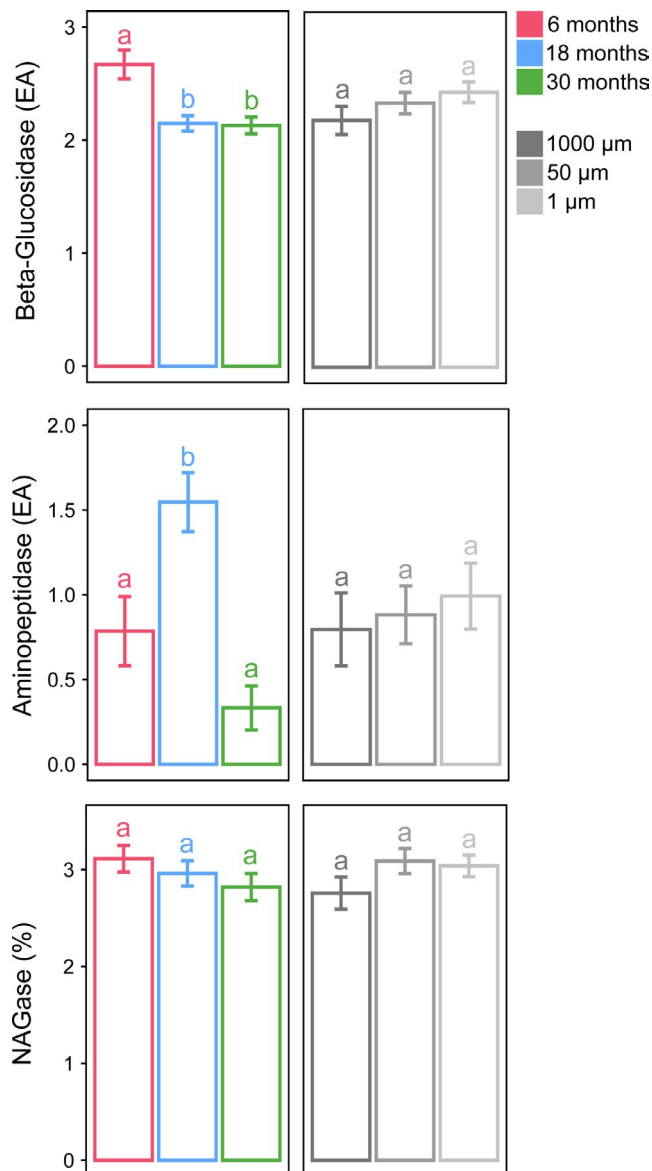


**FIGURE 6** Enzyme activities (pmol/min/g dry weight = EA) (mean  $\pm$  SE) depending on incubation time (6, 18 and 30 months) or mesh size (1000, 50 and 1  $\mu$ m); bars that do not share similar letters denote statistical significance ( $p < .05$ )

### 3.4 | Mass loss from fungal necromass

Asymptotic decay modelling revealed that the mass loss from fungal necromass depended on both mesh size and time. The decay constants, which are characteristic earlier mass loss, were an order of magnitude lower for both the 50 and 1  $\mu$ m mycobags ( $k = -0.43$  and  $k = -0.50$ , respectively) than for the 1000  $\mu$ m mycobags ( $k = -5.65$ ; Figure 7). By contrast, the asymptote values, which are associated with later mass loss, was 1.5 times higher for the 1000  $\mu$ m mycobags than for either the 50  $\mu$ m or the 1  $\mu$ m mycobags. The mass remaining in the 1000  $\mu$ m mycobags was stable at  $\sim 12\%$  in all three harvests, while the mass remaining in both the 50  $\mu$ m and 1  $\mu$ m mycobags was significantly lower ( $\sim 7\%$ ) in both the second and third harvests (Figure S4, Table S6).

## 4 | DISCUSSION

Similar to previous studies demonstrating rapid decomposition of dead fungal mycelia, we found that 85% of the initial fungal necromass was decomposed after 6 months of incubation in forest soil (Brabcová et al., 2016, 2018; Certano et al., 2018; Drigo et al., 2012; Fernandez & Kennedy, 2018; Fernandez & Koide, 2012, 2014). However, we also found that 7%–13% of the initial fungal necromass was still present after 30 months of decomposition. Despite the fungal necromass we used having a relatively low C/N ratio (C/N = 13) and no apparent melanisation, a very stable fraction was retained, which aligns with long-term necromass incubations conducted by Fernandez et al. (2019). The continual change in microbial community composition on fungal necromass over the 30 months of sampling matched with similar changes in microbial decomposer composition that have been observed during the initial stages (i.e., 0–5 months) of fungal necromass degradation (Beidler et al., 2020; Brabcová et al., 2016, 2018; Fernandez & Kennedy, 2018). This suggests that fungal

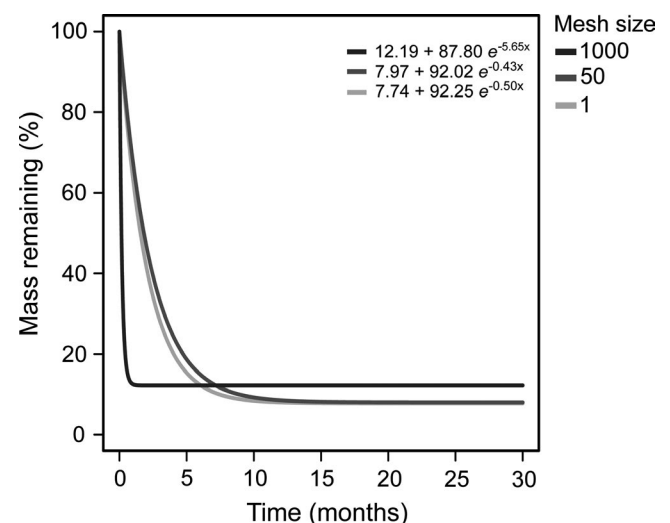


**FIGURE 7** Asymptotic nonlinear exponential decay model fits for each mesh size treatment

necromass remains an active "hotspot" (sensu Brabcová et al., 2016) of microbial colonisation well past its early stages of rapid mass loss. In terms of resource utilisation, we did observe an overall decline in enzyme activity associated with C acquisition from necromass during the course of the incubation, but we did not see more gradual declines in enzymes associated with N acquisition. Instead, the two N acquisition enzymes showed contrasting patterns, which may reflect differential retention times of different compounds in degrading fungal necromass (Certano et al., 2018; Fernandez & Koide, 2012; Fernandez, et al., 2019; Ryan et al., 2020). Consistent with our prediction, we found that root presence had contrasting effects on the initial versus later stages of fungal necromass mass loss. Specifically, we found root presence hastened the initial loss of mass from fungal necromass, but that the mass remaining at later time points was significantly higher in the treatment in which roots and their associated mycorrhizal fungal symbionts were most abundant.

The initial dominance of the bacterial communities on decomposing fungal necromass by the classes Bacteroidetes and Proteobacteria at 6 months of incubation aligned well with previous studies (Beidler et al., 2020; Brabcová et al., 2016, 2018; Fernandez & Kennedy, 2018). However, both of these classes declined after 18 months of incubation and were replaced by classes Bacilli and Acidobacteria. This higher level taxonomic shift mirrored in a functional shift in bacterial community composition over the course of the incubation, with bacteria classified as copiotrophic consistently decreasing and those classified as oligotrophic steadily increasing. These changes correspond well with the increasing limitation of C and N accessibility during the late stages of fungal necromass decomposition (Hu et al., 1999). The genera *Chitinophaga*, *Devosia*, *Mucilagibacter*, *Pedobacter*, *Pseudomonas* and *Variovorax* have been previously shown to be the most abundant bacteria colonising fungal necromass during the first five months of degradation (Brabcová et al., 2016, 2018; Fernandez & Kennedy, 2018). Similarly, we found those same bacterial genera to be highly abundant after 6 months of decomposition. Both *Chitinophaga* and *Pedobacter* have been described as efficient chitin degraders, which suggests they play an active role in the decomposition of this N-containing polymer in fungal necromass (Gordon et al., 2009; Janssen, 2006; Larsbrink et al., 2017; McKee et al., 2019). Consistent with the higher lability of chitin relative to other cell wall components (Fernandez & Koide, 2012), these two bacterial genera were strongly associated with only the first sampling time in our study and then mainly replaced by *Bacillus* and *Paenibacillus*. *Bacillus* and *Paenibacillus* are also relatively common bacterial genera in forest soils, where they have a major role in OM decomposition (López-Mondéjar et al., 2019). Numerous studies using both genomics and enzymatic approaches have revealed that *Bacillus* and *Paenibacillus* have very efficient lignocellulosic degradation mechanisms (Orencio-Trejo et al., 2016; Shin et al., 2012; Song et al., 2014; Woo et al., 2014; Yuki et al., 2014). The significant negative correlations we found between fungal necromass remaining and the relative abundance of *Paenibacillus* provide further support for a key role of this bacterial genus in fungal necromass decomposition. Collectively, our results suggest that early stage of fungal

necromass decomposition are dominated by copiotrophic bacteria degrading the labile compound pool in dead mycelia. In contrast, the later stages of fungal necromass decomposition are composed of bacterial communities with higher OM degradation capacities that are well equipped to utilise the remaining recalcitrant fractions of fungal necromass.

For the fungal communities present on decomposing necromass, members of the Mucorales, particularly the genus *Mucor*, were extremely dominant at all three sampling times. Those results contrast with other studies in which the fungal communities on dead fungal mycelia are mostly dominated by saprotrophs from the phylum Ascomycota (Beidler et al., 2020; Brabcová et al., 2016, 2018; Maillard et al., 2020) or members of the genus *Mortierella* and Basidiomycota ECM fungi (Fernandez & Kennedy, 2018). Most of these studies were conducted for short or medium incubation periods and in temperate ecosystems. Collectively, these results suggest that the genus *Mucor* is principally associated with the late stage of necromass decomposition in boreal forest soils where it is commonly found but its abundance is generally low (Santalahti et al., 2016). Consistent with that possibility, a recent meta-analysis of Vivel and Bhatnagar (2019) described *Mucor* as a middle- and late-stage litter decomposer genus, although Osono (2019) found that members of the Mucoromycota generated insignificant changes of leaf litter chemistry during decomposition. Taken together, these results suggest that in forest ecosystems *Mucor* might act more prominently as decomposers of fungal necromass than real plant OM degraders. This possibility is supported by the significant negative correlation we found between the amount of fungal mass remaining in the relative abundance of *Mucor*. Moreover, the ability of *Mucor* species to degrade fungal cell walls, and chitin in particular, has been described extensively (Krishna & Mohan, 2017; Rast et al., 1991).

At the same study site using the same mesh bag treatments as this study, but instead filled with organic soil, Sietio et al. (2019) found *Mortierella* to be among the most abundant fungal saprotroph coloniser along with ECM fungi in the genera *Lactarius*, *Piloderma* and *Tylospora*. By contrast, in our study, *Mucor* and *Penicillium* were the most abundant saprotrophic fungi colonising the mycobags. Among ECM fungal species, *Cortinarius* was the dominant ECM species colonising the fungal necromass, but *Lactarius*, the dominant ECM fungal genus in soils at this site (Santalahti et al. 2016), was absent from mycobags. Sietio et al. (2019) also revealed that Acidobacteria, Actinobacteria and Alpha-proteobacteria dominated the bacterial communities of organic soil-filled mesh bags whereas we found that the Bacteroidetes, Gamma-proteobacteria and Firmicutes were most commonly associated with fungal necromass. Collectively, these results suggest that the microbial communities associated with fungal necromass differ from those present on other SOM types, further confirming the environmental filter of fungal necromass for decomposer community structure that has been previously described in the literature (Beidler et al., 2020; Brabcová et al., 2016, 2018; Fernandez & Kennedy, 2018).

Analysing the ITS2 sequences for those belonging to plants confirmed that 50 µm and 1 µm mycobags almost entirely eliminated

root presence by comparison with the 1000  $\mu\text{m}$  bags (Figure S5, Table S6). Interestingly, during the initial stage of decomposition, fungal necromass degradation rates were higher in the 1000  $\mu\text{m}$  mycobags compared with the 50  $\mu\text{m}$  mycobags. In the context of a rhizosphere priming hypothesis, these results might be explained by the asynchronicity between the colonisation of the roots and the root-associated fungi in the mycobags. Indeed, root presence was reported at 6 months in the 1000  $\mu\text{m}$  mycobags; however, in parallel, the presence of the root-associated fungi was extremely low at this time point (i.e., ECM, ERM and endophytic fungi). Contrary to our expectations, however, we found that 50  $\mu\text{m}$  mycobags were also significantly depleted in all the fungal guilds associated with roots, notably both ECM and ERM fungi. The limitation of these mycorrhizal fungi appeared to be functionally significant, as the relative abundances of *Amanita*, *Inocybe*, *Piloderma*, and *Melinomyces* were all positively correlated with the amount of fungal necromass remaining. This finding is consistent with a larger literature indicating that ECM fungi slow OM decomposition by competing with free-living saprotrophic microorganisms, a phenomenon known as the "Gadgil effect". (Fernandez & Kennedy, 2016; Fernandez, See, et al., 2019). Previous experimental work in this system has also shown that the presence of root-produced tannins inhibits fungal necromass decomposition (Adamczyk, Sietiö, Biasi, et al., 2019). Because both roots and their symbiotic fungi were dramatically reduced in the 50  $\mu\text{m}$  mycobags yet abundant in the 1000  $\mu\text{m}$  mycobags, distinguishing the effects of the root-associated fungi and the root tannins on the fungal necromass decomposition rates in our study was not possible. Moving forward, experiments are needed to decipher the proportional contribution of these two important ecological mechanisms to slowing necromass decomposition, potentially using tree species with contrasting tannin production in their root systems (Hättenschwiler et al., 2019). Also contrary to our expectations, we observed equally high fungal richness in 1  $\mu\text{m}$  mycobags as in the 50  $\mu\text{m}$  mycobags, indicating that fungi were able to colonise the 1  $\mu\text{m}$  mesh size treatment. This result, although inconsistent with other studies showing that fungi are typically excluded by 1  $\mu\text{m}$  mesh sizes (Teste et al., 2006), was supported by the strikingly similar decomposition dynamics and enzymatic profiles between the 50  $\mu\text{m}$  and 1  $\mu\text{m}$  mycobags. Fungal colonisation in the 1  $\mu\text{m}$  mesh treatment might be linked to the extensive incubations in this study, allowing time for fungi to enter the bags via hyphae. Additionally, because fungal necromass represents a very high-quality OM type, we suspect that the fungi may have invested strongly in penetrating the 1  $\mu\text{m}$  mesh to access this resource. Given this colonisation pattern, our conclusions about the specific role of bacteria in fungal necromass degradation are limited.

The enzymatic activities we measured on decomposing fungal necromass suggest that this substrate remains of active site of microbial activity even when mass loss is negligible. In the only other study to measure enzymes associated with decomposing fungal necromass, Brabcová et al. (2016) documented that  $\beta$ -glucosidase activity was similarly high at nine and 23 weeks after soil incubation. Here, we found that the activity of this enzyme declines over

longer incubation periods, which is consistent its targeting of more labile forms of C. In interesting opposition to our hypothesis, the activity of leucine-aminopeptidase spiked after 18 months of decomposition. This suggests that proteins and peptides associated with fungal necromass may have an initially low accessibility relative to other cellular components. Consistent with this possibility, activity of leucine-aminopeptidase during the initial stages of necromass decomposition was lower than other enzymes measured by Brabcová et al., (2016). The lack of change in N-acetylglucosaminidase activity over time may reflect the fact that chitin decomposes quickly relative to other fungal cellular components (Fernandez & Koide, 2012), so our later sampling may have missed the peak activity of this enzyme. Alternatively, the even activity of N-acetylglucosaminidase throughout incubation time may reflect the continual degradation of decomposer fungi that are themselves being decomposed post necromass colonisation and senescence. We did not observe higher enzymatic activities in the treatment which included roots, which confirms the lack of a rhizosphere priming effect in the later stages of the decomposition of fungal necromass. However, we suspect this phenomenon was probably present in the early stages of fungal necromass decomposition, as the presence of roots has been consistently shown to stimulate microbial OM decomposition in both empirical (Brzostek et al., 2015) and modelling studies (Moore et al., 2015).

Finally, we acknowledge that the use of different mesh sizes to control the access of plant roots and microbial guilds has some important caveats. It has been reported that microparameters might vary within the mesh bags depending on their mesh size, potentially having consequences on the OM decomposition dynamics (Beidler & Pritchard, 2017). Additionally, soil fauna, potentially important for fungal necromass decomposition, has limited access to the 50  $\mu\text{m}$  and 1  $\mu\text{m}$  mycobags by comparison with the 1000  $\mu\text{m}$  mesh size (Frouz et al., 2015; González & Seastedt, 2001). New experiments are necessary to further our knowledge about the role of the root and root-associated microbes in fungal necromass decomposition. For example, trenching experiments, which eliminate roots but allow the direct movement of fauna as well as soil water fluxes may help in better understanding necromass decomposition dynamics (Fernandez et al., 2019). Complementarily, microbial isolations directly from necromass and their reconstruction in simplified axenic mesocosms represent another promising alternative (Durán et al., 2018).

## 5 | CONCLUSIONS

This study provides the first in-depth characterisation of the structure of microbial communities associated with decomposing fungal necromass at time scales beyond five months of incubation. Understanding the taxonomic and functional composition of these communities is essential for better understanding how the more recalcitrant fractions of fungal necromass, which disproportionately contribute to stable soil OM (Fernandez et al., 2019; Ryan et al., 2020), decompose and cycle in forest soils. In addition to identifying long-term shifts in microbial community composition, we also demonstrate that the activity

of enzymes involved in C and N acquisition from necromass continue to change at multiyear time scales. This suggests that both the C and N resources in fungal necromass remain active targets of microbial degradation well beyond the period of rapid initial mass loss. Finally, our reanalysis of fungal necromass mass loss rates indicates that plant roots in boreal forests have a more complex role in fungal necromass decomposition than previously recognised. Specifically, our results suggest that the presence of roots initially augment but then later retard rates of fungal necromass decomposition.

## ACKNOWLEDGEMENTS

FM was awarded a PhD fellowship by the Région Lorraine (n°12000498) and the French National Research Agency (ANR) as part of the “Investissements d’Avenir” program (ANR-11-LABX-0002-01, Laboratory of Excellence ARBRE). Dr Outi-Maaria Sietiö is acknowledged for skillful assistance in the enzyme analyses. We also acknowledge the constructive comments by three anonymous reviewers.

## AUTHOR CONTRIBUTIONS

J.H. designed the study. J.H., B.A. and F.M. carried out the experiment. F.M., M.B. and P.K. performed the data analyses. F.M. wrote the manuscript with support from P.K., J.H., B.A. and M.B. All the authors contributed to the final manuscript.

## DATA AVAILABILITY STATEMENT

Raw.fastq files for each sample and associated metadata (e.g., mass loss) were deposited in the NCBI Short Read Archive as accession PRJNA632557. The other metadata (e.g., enzymatic data) are presented in Table S7 with the same sample identification code than the sequencing data.

## ORCID

François Maillard  <https://orcid.org/0000-0002-2144-5629>

## REFERENCES

- Adamczyk, B., Sietiö, O. M., Biasi, C., & Heinonsalo, J. (2019). Interaction between tannins and fungal necromass stabilises fungal residues in boreal forest soils. *New Phytologist*, *223*, 16–21.
- Adamczyk, B., Sietiö, O., Straková, P., Prommer, J., Wild, B., Hanger, M., Pihlatie, M., Fritze, H., Richter, A., & Heinonsalo, J. (2019). Plant roots increase both decomposition and stable organic matter formation in boreal forest soil. *Nature Communications*, *10*, 3982.
- Akroume, E., Maillard, F., Bach, C., Hossann, C., Brechet, C., Angeli, N., Zeller, B., Saint-André, L., & Buée, M. (2019). First evidences that the ectomycorrhizal fungus *Paxillus involutus* mobilises nitrogen and carbon from saprotrophic fungus necromass. *Environmental Microbiology*, *21*, 197–208.
- Altschul, S. F., Gish, W., Miller, W., Myers, E. W., & Lipman, D. J. (1990). Basic local alignment search tool. *Journal of Molecular Biology*, *215*, 403–410.
- Beidler, K. V., Phillips, R. P., Andrews, E., Maillard, F., Mushinski, R. M., & Kennedy, P. G. (2020). Substrate quality drives fungal necromass decay and decomposer community structure under contrasting vegetation types. *Journal of Ecology*, *108*, 1845–1859.
- Beidler, K., & Pritchard, S. (2017). Maintaining connectivity: understanding the role of root order and mycelial networks in fine root decomposition of woody plants. *Plant and Soil*, *420*, 19–36.
- Berg, B. (2014). Decomposition patterns for foliar litter – A theory for influencing factors. *Soil Biology and Biochemistry*, *78*, 222–232.
- Bödeker, I. T. M., Clemmensen, K. E., de Boer, W., Martin, F., Olson, A., & Lindahl, B. D. (2014). Ectomycorrhizal *Cortinarius* species participate in enzymatic oxidation of humus in northern forest ecosystems. *New Phytologist*, *203*, 245–256.
- Brabcová, V., Nováková, M., Davidova, A., & Baldrian, P. (2016). Dead fungal mycelium in forest soil represents a decomposition hotspot and a habitat for a specific microbial community. *New Phytologist*, *210*, 1369–1381.
- Brabcová, V., Štursová, M., & Baldrian, P. (2018). Nutrient content affects the turnover of fungal biomass in forest topsoil and the composition of associated microbial communities. *Soil Biology and Biochemistry*, *118*, 187–198.
- Brzostek, E. R., Dragoni, D., Brown, Z. A., & Phillips, R. P. (2015). Mycorrhizal type determines the magnitude and direction of root-induced changes in decomposition in a temperate forest. *New Phytologist*, *206*(4), 1274–1282.
- Buée, M., Courty, P. E., Mignot, D., & Garbaye, J. (2007). Soil niche effect on species diversity and catabolic activities in an ectomycorrhizal fungal community. *Soil Biology and Biochemistry*, *39*, 1947–1955.
- Caporaso, J. G., Lauber, C. L., Walters, W. A., Berg-Lyons, D., Huntley, J., Fierer, N., Owens, S. M., Betley, J., Fraser, L., Bauer, M., Gormley, N., Gilbert, J. A., Smith, G., & Knight, R. (2012). Ultra-high-throughput microbial community analysis on the Illumina HiSeq and MiSeq platforms. *ISME Journal*, *6*, 1621–1624.
- Certano, A. K., Fernandez, C. W., Heckman, K. A., & Kennedy, P. G. (2018). The afterlife effects of fungal morphology: Contrasting decomposition rates between diffuse and rhizomorphic necromass. *Soil Biology and Biochemistry*, *126*, 76–81.
- Clemmensen, K. E., Bahr, A., Ovaskainen, O., Dahlberg, A., Ekblad, A., Wallander, H., Stenlid, J., Finlay, R. D., Wardle, D. A., & Lindahl, B. D. (2013). Roots and associated fungi drive long-term carbon sequestration in boreal forest. *Science*, *340*, 1615–1618.
- Cools, N., Vesterdal, L., De Vos, B., Vanguelova, E., & Hansen, K. (2014). Tree species is the major factor explaining C: N ratios in European forest soils. *Forest Ecology and Management*, *311*, 3–16.
- Courty, P.-E., Pritsch, K., Schloter, M., Hartmann, A., & Garbaye, J. (2005). Activity profiling of ectomycorrhizal communities in two forest soils using multiple enzymatic tests. *New Phytologist*, *167*, 309–319.
- Crowther, T. W., Todd-Brown, K. E. O., Rowe, C. W., Wieder, W. R., Carey, J. C., Machmuller, M. B., Snoek, B. L., Fang, S., Zhou, G., Allison, S. D., Blair, J. M., Bridgman, S. D., Burton, A. J., Carrillo, Y., Reich, P. B., Clark, J. S., Classen, A. T., Dijkstra, F. A., Elberling, B., ... Bradford, M. A. (2016). Quantifying global soil carbon losses in response to warming. *Nature*, *540*, 104–108.
- Drigo, B., Anderson, I. C., Kannangara, G. S. K., Cairney, J. W. G., & Johnson, D. (2012). Rapid incorporation of carbon from ectomycorrhizal mycelial necromass into soil fungal communities. *Soil Biology and Biochemistry*, *49*, 4–10.
- Durán, P., Thiergart, T., Garrido-Oter, R., Agler, M., Kemen, E., Schulze-Lefert, P., & Hacquard, S. (2018). Microbial interkingdom interactions in roots promote *Arabidopsis* survival. *Cell*, *175*, 973–983.e14.
- Edgar, R. C. (2013). UPARSE: Highly accurate OTU sequences from microbial amplicon reads. *Nature Methods*, *10*, 996–998.
- Ekblad, A., Wallander, H., Godbold, D. L., Cruz, C., Johnson, D., Baldrian, P., Björk, R. G., Epron, D., Kieliszewska-Rokicka, B., Kjoller, R., Kraigher, H., Matzner, E., Neumann, J., & Plassard, C. (2013). The production and turnover of extramatrical mycelium of ectomycorrhizal fungi in forest soils: role in carbon cycling. *Plant and Soil*, *366*, 1–27.
- Fernandez, C. W., Heckman, K., Kolka, R., & Kennedy, P. G. (2019). Melanin mitigates the accelerated decay of mycorrhizal necromass with peatland warming. *Ecology Letters*, *22*, 498–505.
- Fernandez, C. W., & Kennedy, P. G. (2016). Revisiting the ‘Gadgil effect’: Do interguild fungal interactions control carbon cycling in forest soils? *New Phytologist*, *209*, 1382–1394.



- Fernandez, C. W., & Kennedy, P. G. (2018). Melanization of mycorrhizal fungal necromass structures microbial decomposer communities. *Journal of Ecology*, *106*, 468–479.
- Fernandez, C. W., & Koide, R. T. (2012). The role of chitin in the decomposition of ectomycorrhizal fungal litter. *Ecology*, *93*, 24–28.
- Fernandez, C. W., & Koide, R. T. (2014). Initial melanin and nitrogen concentrations control the decomposition of ectomycorrhizal fungal litter. *Soil Biology and Biochemistry*, *77*, 150–157.
- Fernandez, C. W., Langley, J. A., Chapman, S., McCormack, M. L., & Koide, R. T. (2016). The decomposition of ectomycorrhizal fungal necromass. *Soil Biology and Biochemistry*, *93*, 38–49.
- Fernandez, C. W., See, C. R., & Kennedy, P. G. (2019). Decelerated carbon cycling by ectomycorrhizal fungi is controlled by substrate quality and community composition. *New Phytologist*, *226*(2), 569–582. <https://doi.org/10.1111/nph.16269>.
- Frey, S. D. (2019). Mycorrhizal fungi as mediators of soil organic matter dynamics. *Annual Review of Ecology, Evolution, and Systematics*, *50*, 237–259.
- Frouz, J., Roubícková, A., Hedenec, P., & Tajovský, K. (2015). Do soil fauna really hasten litter decomposition? A meta-analysis of enclosure studies. *European Journal of Soil Biology*, *68*, 18–24.
- González, G., & Seastedt, T. R. (2001). Soil fauna and plant litter decomposition in tropical and subalpine forests. *Ecology*, *82*, 955–964.
- Gordon, N. S., Valenzuela, A., Adams, S. M., Ramsey, P. W., Pollock, J. L., Holben, W. E., & Gannon, J. E. (2009). *Pedobacter nyackensis* sp nov., *Pedobacter alluvionis* sp nov and *Pedobacter borealis* sp nov., isolated from Montana flood-plain sediment and forest soil. *International Journal of Systematic and Evolutionary Microbiology*, *59*, 1720–1726.
- Hari, P., & Kulmala, M. (2005). Station for measuring ecosystem-atmosphere relations (SMEAR II). *Boreal Environmental Research*, *10*, 315–322.
- Hättenschwiler, S., Sun, T., & Coq, S. (2019). The chitin connection of polyphenols and its ecosystem consequences. *New Phytologist*, *223*, 5–7.
- Heinonsalo, J., Kabiersch, G., Niemi, R. M., Simpanen, S., Ilvesniemi, H., Hofrichter, M., Hatakka, A., & Steffen, K. T. (2012). Filter centrifugation as a sampling method for miniaturisation of extracellular fungal enzyme activity measurements in solid media. *Fungal Ecology*, *5*, 261–269.
- Heinonsalo, J., Sun, H., Santalahti, M., Backlund, K., Hari, P., & Pumpanen, J. (2015). Evidence on the ability of mycorrhizal genus *Piloderma* to use organic nitrogen and deliver it to Scots pine. *PLoS One*, *10*, e0131561.
- Hodge, A., Alexander, I. J., & Gooday, G. W. (1995). Chitinolytic enzymes of pathogenic and ectomycorrhizal fungi. *Mycological Research*, *99*, 935–941.
- Högberg, P., Näsholm, T., Franklin, O., & Högberg, M. (2017). Tamm review: On the nature of the nitrogen limitation to plant growth in Fennoscandian boreal forests. *Forest Ecology and Management*, *403*, 161–185.
- Hu, S. J., van Bruggen, A. H. C., & Grünwald, N. J. (1999). Dynamics of bacterial populations in relation to carbon availability in a residue-amended soil. *Applied Soil Ecology*, *13*, 21–30.
- Ihrmark, K., Bodeker, I. T. M., Cruz-Martinez, K., Friberg, H., Kubartova, A., Schenck, J., Strid, Y., Stenlid, J., Brandstrom-Durling, M., Clemmensen, K. E., & Lindahl, B. D. (2012). New primers to amplify the fungal ITS2 region—Evaluation by 454-sequencing of artificial and natural communities. *FEMS Microbiology Ecology*, *82*, 666–677.
- Ilvesniemi, H., Giesler, R., van Hees, P., Magnusson, T., & Melkerud, P. A. (2000). General description of the sampling techniques and the sites investigated in the Fennoscandinavian podzolisation project. *Geoderma*, *94*, 109–123.
- Janssen, P. H. (2006). Identifying the dominant soil bacterial taxa in libraries of 16S rRNA and 16S rRNA genes. *Applied and Environmental Microbiology*, *72*, 1719–1728.
- Koide, R. T., Fernandez, C., & Malcolm, G. (2014). Determining place and process: Functional traits of ectomycorrhizal fungi that affect both community structure and ecosystem function. *New Phytologist*, *201*, 433–439.
- Koide, R. T., & Malcolm, G. M. (2009). N concentration controls decomposition rates of different strains of ectomycorrhizal fungi. *Fungal Ecology*, *2*, 197–202.
- Kõljalg, U., Nilsson, R. H., Abarenkov, K., Tedersoo, L., Taylor, A. F. S., Bahram, M., Bates, S. T., Bruns, T. D., Bengtsson-Palme, J., Callaghan, T. M., Douglas, B., Drenkhan, T., Eberhardt, U., Dueñas, M., Grebenc, T., Griffith, G. W., Hartmann, M., Kirk, P. M., Kohout, P., ... Larsson, K.-H. (2013). Towards a unified paradigm for sequence-based identification of fungi. *Molecular Ecology*, *22*(21), 5271–5277.
- Krishna, M. P., & Mohan, M. (2017). Litter decomposition in forest ecosystems: A review. *Energy, Ecology and Environment*, *2*(4), 236–249.
- Kuyper, T. W. (2017). Carbon and energy sources of mycorrhizal fungi: obligate symbionts or latent saprotrophs? In: *Mycorrhizal mediation of soil* (pp. 357–374).
- Kuzyakov, Y. (2010). Priming effects: interactions between living and dead organic matter. *Soil Biology and Biochemistry*, *42*, 1363–1371.
- Kyaschenko, J., Clemmensen, K. E., Hagenbo, A., Karlton, E., & Lindahl, B. D. (2017). Shift in fungal communities and associated enzyme activities along an age gradient of managed *Pinus sylvestris* stands. *ISME Journal*, *11*, 863–875.
- Kyaschenko, J., Clemmensen, K. E., Karlton, E., & Lindahl, B. D. (2017). Below-ground organic matter accumulation along a boreal forest fertility gradient relates to guild interaction within fungal communities. *Ecology Letters*, *20*, 1546–1555.
- Larsbrink, J., Tuveng, T. R., Pope, P. B., Bulone, V., Eijsink, V. G., Brumer, H., & McKee, L. S. (2017). Proteomic insights into mannan degradation and protein secretion by the forest floor bacterium *Chitinophaga pinensis*. *Journal of Proteomics*, *156*, 63–74.
- Lehmann, J., & Kleber, M. (2015). The contentious nature of soil organic matter. *Nature*, *528*, 60–68.
- Li, S., Deng, Y., Wang, Z., Zhang, Z., Kong, X., Zhou, W., Yi, Y., & Qu, Y. (2020). Exploring the accuracy of amplicon-based internal transcribed spacer markers for a fungal community. *Molecular Ecology Resources*, *20*, 170–184.
- Liang, C., Amelung, W., Lehmann, J., & Kästner, M. (2019). Quantitative assessment of microbial necromass contribution to soil organic matter. *Global Change Biology*, *25*, 3578–3590.
- López-Mondéjar, R., Algora, C., & Baldrian, P. (2019). Lignocellulolytic systems of soil bacteria: A vast and diverse tool box for biotechnological conversion processes. *Biotechnology Advances*, *37*, 1073742.
- Maillard, F., Didion, M., Fauchery, L., Bach, C., & Buée, M. (2018). N-Acetylglucosaminidase activity, a functional trait of chitin degradation, is regulated differentially within two orders of ectomycorrhizal fungi: Boletales and Agaricales. *Mycorrhiza*, *28*, 391–397.
- Maillard, F., Schilling, J., Andrews, E., Schreiner, K. M., & Kennedy, P. (2020). Functional convergence in the decomposition of fungal necromass in soil and wood. *FEMS Microbiology Ecology*, *96*, fuz209.
- McKee, L. S., Martínez-Abad, A., Ruthes, A. C., Vilaplana, F., & Brumer, H. (2019). Focused metabolism of  $\beta$ -Glucans by the soil *Bacteroidetes* species *Chitinophaga pinensis*. *Applied and Environmental Microbiology*, *85*(2), e02231–e2318.
- Moore, J. A., Jiang, J., Patterson, C. M., Mayes, M. A., Wang, G., & Classen, A. T. (2015). Interactions among roots, mycorrhizas and free-living microbial communities differentially impact soil carbon processes. *Journal of Ecology*, *103*(6), 1442–1453.
- Mucha, J., Dahm, H., Strzelczyk, E., & Werner, A. (2006). Synthesis of enzymes connected with mycoparasitism by ectomycorrhizal fungi. *Archives of Microbiology*, *185*, 69–77.
- Näsholm, T., Kielland, K., & Ganeteg, U. (2009). Uptake of organic nitrogen by plants. *New Phytologist*, *182*, 31–48.

- Nguyen, N. H., Song, Z., Bates, S. T., Branco, S., Tedersoo, L., Menke, J., Schilling, J. S., & Kennedy, P. G. (2016). FUNGuild: An open annotation tool for parsing fungal community datasets by ecological guild. *Fungal Ecology*, *20*, 241–248.
- Nicolás, C., Martin-Bertelsen, T., Floudas, D., Bentzer, J., Smits, M., Johansson, T., Troein, C., Persson, P., & Tunlid, A. (2019). The soil organic matter decomposition mechanisms in ectomycorrhizal fungi are tuned for liberating soil organic nitrogen. *The ISME Journal*, *13*, 977–988.
- Oksanen, J., Blanchet, F. G., Kindt, R., Legendre, P., Minchin, P. R., O'hara, R. B., Simpson, G. L., Solymos, P., Stevens, M. H., & Wagner, H. (2013). *vegan: Community Ecology Package, version 2.0-7*. R package. Retrieved from <http://CRAN.R-project.org/package=vegan>.
- Orencio-Trejo, M., De la Torre-Zavala, S., Rodriguez-Garcia, A., Aviles-Arnaut, H., & Gastelum-Arellanez, A. (2016). Assessing the performance of bacterial cellulases: the use of *Bacillus* and *Paenibacillus* strains as enzyme sources for lignocellulose saccharification. *BioEnergy Research*, *9*, 1023–1033.
- Osono, T. (2019). Functional diversity of ligninolytic fungi associated with leaf litter decomposition. *Ecological Research*, *35*, 30–43.
- Pan, Y., Birdsey, R. A., Fang, J., Houghton, R., Kauppi, P. E., Kurz, W. A., Phillips, O. L., Shvidenko, A., Lewis, S. L., Canadell, J. G., Ciais, P., Jackson, R. B., Pacala, S. W., McGuire, A. D., Piao, S., Rautiainen, A., Sitch, S., & Hayes, D. (2015). A large and persistent carbon sink in the world's forests. *Science*, *333*, 988–993.
- Pruesse, E., Quast, C., Knittel, K., Fuchs, B. M., Ludwig, W., Peplies, J., & Glöckner, F. O. (2007). SILVA: A comprehensive online resource for quality checked and aligned ribosomal RNA sequence data compatible with ARB. *Nucleic Acids Research*, *35*, 7188–7196.
- R Core Team (2016). *R: A language and environment for statistical computing*. R Foundation for Statistical Computing.
- Rajala, T., Peltoniemi, M., Pennanen, T., & Mäkipää, R. (2012). Fungal community dynamics in relation to substrate quality of decaying Norway spruce (*Picea abies* [L.] Karst.) logs in boreal forests. *FEMS Microbiology and Ecology*, *81*, 494–505.
- Rajala, T., Tuomivirta, T., Pennanen, T., & Mäkipää, R. (2015). Habitat models of wood-inhabiting fungi along a decay gradient of Norway spruce logs. *Fungal Ecology*, *18*, 48–55.
- Rast, D. M., Horsch, M., Furter, R., & Gooday, G. W. (1991). A complex chitinolytic system in exponentially growing mycelium of *Mucor rouxii*—Properties and function. *Journal of General Microbiology*, *137*, 2797–2810.
- Rineau, F., Roth, D., Shah, F., Smits, M., Johansson, T., Canback, B., Olsen, P. B., Persson, P., Grell, M. N., Lindquist, E. et al (2012). The ectomycorrhizal fungus *Paxillus involutus* converts organic matter in plant litter using a trimmed brown-rot mechanism involving Fenton chemistry. *Environmental Microbiology*, *14*, 1477–1487.
- Ryan, M. E., Schreiner, K. M., Swenson, J. T., Gagne, J., & Kennedy, P. G. (2020). Rapid changes in the chemical composition of degrading ectomycorrhizal fungal necromass. *Fungal Ecology*, *45*, 100922.
- Santalahti, M., Sun, H., Jumpponen, A., Pennanen, T., & Heinonsalo, J. (2016). Vertical and seasonal dynamics of fungal communities in boreal Scots pine forest soil. *FEMS Microbiology Ecology*, *92*, fiw170.
- Schweigert, M., Herrmann, S., Miltner, A., Fester, T., & Kastner, M. (2015). Fate of ectomycorrhizal fungal biomass in a soil bioreactor system and its contribution to soil organic matter formation. *Soil Biology and Biochemistry*, *88*, 120–127.
- Shin, S. H., Kim, S., Kim, J. Y., Song, H. Y., Cho, S. J., Kim, D. R., Lee, K. I., Lim, H. K., Park, N. J., Hwang, I. T., & Yang, K. S. (2012). Genome sequence of *Paenibacillus terrae* HPL-003, a xylanase-producing bacterium isolated from soil found in forest residue. *Journal of Bacteriology*, *194*, 1266.
- Sietiö, O.-M., Santalahti, M., Putkinen, A., Adamczyk, S., Sun, H., & Heinonsalo, J. (2019). Restriction of plant roots in boreal forest organic soils affects the microbial community but does not change the dominance from ectomycorrhizal to saprotrophic fungi. *FEMS Microbiology Ecology*, *95*, fiz133.
- Siletti, C. E., Zeiner, C. A., & Bhatnagar, J. M. (2017). Distributions of fungal melanin across species and soils. *Soil Biology and Biochemistry*, *113*, 285–293.
- Song, H. Y., Lim, H. K., Kim, D. R., Lee, K. I., & Hwang, I. T. (2014). A new bi-modular endo- $\beta$ -1,4-xylanase KRICT PX-3 from whole genome sequence of *Paenibacillus terrae* HPL-003. *Enzyme and Microbial Technology*, *54*, 1–7.
- Sterkenburg, E., Bahr, A., Brandström Durling, M., Clemmensen, K. E., & Lindahl, B. D. (2015). Changes in fungal communities along a boreal forest soil fertility gradient. *New Phytologist*, *207*, 1145–1158.
- Sun, T., Hobbie, S. E., Berg, B., Zhang, H., Wang, Q., Wang, Z., & Hättenschwiler, S. (2018). Contrasting dynamics and trait controls in first-order root compared with leaf litter decomposition. *Proceedings of the National Academy of Sciences USA*, *115*, 10392–10397.
- Teste, F. P., Karst, J., Jones, M. D., Simard, S. W., & Durall, D. M. (2006). Methods to control ectomycorrhizal colonisation: Effectiveness of chemical and physical barriers. *Mycorrhiza*, *17*(1), 51–65.
- Trivedi, P., Wallenstein, M. D., Delgado-Baquerizo, M., & Singh, B. K. (2018). Chapter 3 – Microbial modulators and mechanisms of soil carbon storage. In B. K. Singh (Ed.), *Soil carbon storage* (pp. 73–115). Academic Press.
- UNITE Community (2017). *Full UNITE+INSD dataset*. Version 01.12.2017. UNITE Community.
- Vivelo, S., & Bhatnagar, F. M. (2019). An evolutionary signal to fungal succession during plant litter decay. *FEMS Microbiology Ecology*, *95*(10), fiz145.
- Voříšková, J., & Baldrian, P. (2013). Fungal community on decomposing leaf litter undergoes rapid successional changes. *ISME Journal*, *7*, 477–486.
- Wallander, H., Nilsson, L. O., Hagerberg, D., & Rosengren, U. (2003). Direct estimates of C:N ratios of ectomycorrhizal mycelia collected from Norway spruce forest soils. *Soil Biology and Biochemistry*, *35*, 997–999.
- Wang, C., Wang, X. U., Pei, G., Xia, Z., Peng, B. O., Sun, L., Wang, J., Gao, D., Chen, S., Liu, D., & Dai, W. (2020). Stabilisation of microbial residues in soil organic matter after two years of decomposition. *Soil Biology and Biochemistry*, *141*, 107687.
- Woo, H. L., Hazen, T. C., Simmons, B. A., & DeAngelis, K. M. (2014). Enzyme activities of aerobic lignocellulolytic bacteria isolated from wet tropical forest soils. *Systematic and Applied Microbiology*, *37*, 60–67.
- Yuki, M., Oshima, K., Suda, W., Oshida, Y., Kitamura, K., Iida, T., Hattori, M., & Ohkuma, M. (2014). Draft genome sequence of *Paenibacillus pini* JCM 16418T, isolated from the rhizosphere of pine tree. *Genome Announcements*, *2*, e00210–e00214.

## SUPPORTING INFORMATION

Additional supporting information may be found online in the Supporting Information section.

**How to cite this article:** Maillard F, Kennedy PG, Adamczyk B, Heinonsalo J, Buée M. Root presence modifies the long-term decomposition dynamics of fungal necromass and the associated microbial communities in a boreal forest. *Mol Ecol*. 2021;00:1–15. <https://doi.org/10.1111/mec.15828>